

Available online at www.sciencedirect.com

ScienceDirect

journal homepage: <http://Elsevier.com/locate/radcr>

Cardiac

Cardiac magnetic resonance imaging and a rare case of an atrial myxoma causing an atrial septal defect

Matthew Grant MD^{a,*}, Samuel Douglass DO^a, Eric Roberge MD^a, Eric Shry MD^b

^a Department of Radiology, Madigan Army Medical Center, 9040 Jackson Ave, Tacoma, WA 98431

^b Department of Cardiology, Madigan Army Medical Center, 9040 Jackson Ave, Tacoma, WA 98431

ARTICLE INFO

Article history:

Received 13 March 2017

Received in revised form 15 June 2017

Accepted 3 July 2017

Available online

Keywords:

Cardiac magnetic resonance imaging

Atrial myxoma

Cardiac mass

Echocardiogram

Atrial septal defect

Dyspnea

ABSTRACT

A 40 year-old athletic woman presented with worsening dyspnea on exertion over the preceding several months. Chest radiograph showed borderline cardiomegaly and subsequent echocardiography demonstrated a 5.0-cm left atrial mass as well as left-to-right interatrial shunting through a patent foramen ovale. Cardiac magnetic resonance imaging was performed, which demonstrated signal characteristics consistent with an atrial myxoma. The patient then underwent urgent surgical treatment with good technical and clinical outcome. Histologic examination confirmed an atrial myxoma. Cardiac magnetic resonance imaging was valuable in characterizing the nature of the atrial mass and patent foramen ovale, helping guide the surgical approach.

© 2017 the Authors. Published by Elsevier Inc. under copyright license from the University of Washington. This is an open access article under the CC BY-NC-ND license (<http://creativecommons.org/licenses/by-nc-nd/4.0/>).

Introduction

Cardiac tumors, whether benign or malignant, require prompt diagnostic workup and therapeutic intervention. Transthoracic echocardiography (TTE) is widely available and remains essential in the initial workup of suspected cardiac tumors. However, it has significant limitations, to include limited fields of view of right heart and extracardiac structures, as well as operator and patient dependent factors. Additional imaging with transesophageal echocardiography (TEE) resolves some of these issues, but is invasive and requires sedation. Other imaging

modalities, including computed tomography (CT) and cardiac magnetic resonance (CMR) imaging, are useful in evaluating cardiac tumors. Physicians should be aware that CMR has become increasingly valuable in both establishing a diagnosis and guiding appropriate therapeutic options for confirmed cardiac tumors [1].

The main differential of a left cardiac mass includes “pseudotumors” (eg, thrombus, anatomic variants), followed next by metastatic tumors and then primary cardiac tumors (benign and malignant) [1]. Metastatic tumors (eg, breast, lung, melanoma, lymphoma) are up to 40 times more common than primary cardiac tumors [2]. Primary cardiac tumors are rare,

Competing Interests: None.

* Corresponding author.

E-mail address: matthew.d.grant3.mil@mail.mil (M. Grant).

<https://doi.org/10.1016/j.radcr.2017.07.001>

1930-0433/© 2017 the Authors. Published by Elsevier Inc. under copyright license from the University of Washington. This is an open access article under the CC BY-NC-ND license (<http://creativecommons.org/licenses/by-nc-nd/4.0/>).

and greater than 75% are benign [1]. Of the benign primary tumors, myxomas make up the majority, followed by lipomas, papillary fibroelastomas (the most common valvular tumor), and rhabdomyomas (most common in children), to name a few [1]. Although making up less than 25% of all primary cardiac tumors, malignant sarcomas (angiosarcoma, fibrosarcoma, and rhabdomyosarcomas in children) are the second most common primary cardiac tumor [3]. Pericardial tumors can also mimic primary tumors, the 2 most common being teratomas and mesotheliomas [3]. The therapeutic options for some of these conditions vary widely. CMR helps differentiate benign from malignant tumors by the level of tissue invasion and extracardiac involvement, and thrombus from benign tumors by the presence of enhancement. Furthermore, the tissue type can be better characterized by the degree of sequence-dependent signal intensity.

Case report

A 40-year-old athletic woman presented to her primary care doctor complaining of dyspnea on exertion. The dyspnea had gradually worsened over the preceding months and significantly so over the few days before presentation, occurring after approximately 400 meters of running. She also admitted to audible wheezing, but denied other complaints on review of systems. Her only notable medical history was that her father suffered a myocardial infarction at age 43. Her vital signs and physical examinations, to include heart and lung examinations, were unremarkable. Given these nonspecific findings (wheezing and dyspnea on exertion), her primary care doctor elected to treat her for presumed exercise-induced asthma with albuterol before physical activity. Additionally, she was referred for pulmonary function tests and a chest radiograph.

Her pulmonary function tests revealed normal baseline spirometry. Her chest radiograph was notable for borderline heart enlargement without specific cardiac chamber enlargement. She continued to experience dyspnea on exertion, so an

electrocardiogram (ECG) and TTE were ordered to evaluate her heart enlargement. Her ECG showed normal sinus rhythm, but with a P wave that was both 1.0 mm wide and deep in lead V1, consistent with left atrial abnormality. The TTE displayed normal left ventricular function and ejection fraction. A large left atrial mass, measuring 4.6×2.3 cm (Fig. 1A) and producing moderate functional mitral stenosis was present. Color Doppler imaging showed an atrial septal defect (ASD) with left-to-right interatrial shunting (Fig. 1B). A TEE, left heart catheterization, and CMR were subsequently performed to better characterize the mass and ASD. TEE revealed a normal-sized left atrium containing a multilobulated, heterogeneously echogenic mass (5.1×2.4 cm) attached anterior to the fossa ovalis, extending across the aorto-mitral continuity, and terminating 1.0 cm before the anterior mitral leaflet tip. Furthermore, the previously demonstrated ASD was shown to be a patent foramen ovale (PFO) that opened as the tumor descended into the left ventricle (Fig. 2A and 2B, and supplementary video). The left heart catheterization demonstrated faint calcifications and tumor blush of the mass, as well as atrioventricular and sinoatrial nodal arteries that were larger than usual, possibly supplying blood to the mass. The CMR displayed a well-circumscribed, noninfiltrative mass with a broad-based attachment to the interatrial septum as described above. This mass was mildly intense on T1-weighted imaging, highly intense on T2-weighted imaging, and showed no evidence of fat saturation. The mass showed very mild heterogeneous enhancement on both immediate and delayed post-gadolinium imaging. There was no evidence of malignancy such as a pericardial effusion, extracardiac masses, or pathologically enlarged hilar or mediastinal lymph nodes. Gradient echo CMR imaging redemonstrated the opening of the PFO and interatrial shunting as the attached mass descended into the left ventricle during diastole with excellent visual resolution (Fig. 3A-D).

A multidisciplinary team was convened to include members from the departments of cardiology, cardiothoracic surgery, and diagnostic radiology. Given the diagnostic information above, the mass was most likely benign and consistent with an atrial myxoma, for reasons detailed later. Regardless of the diagnosis,

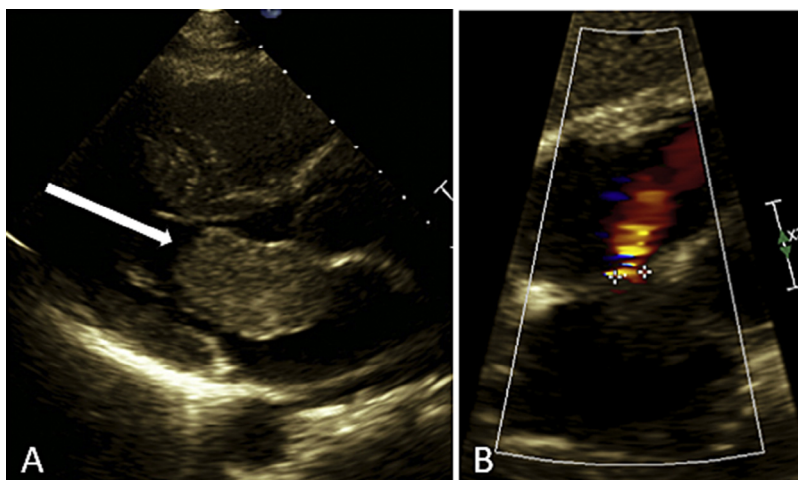


Fig. 1 – Transthoracic echocardiogram. (A) Gray-scale ultrasound image showing the left atrial mass with its distal tip (arrow) descending into the left ventricle during ventricular diastole. (B) Color Doppler image showing directional flow toward the ultrasound transducer and into the right atrium, signifying an atrial septal defect with left-to-right blood flow.

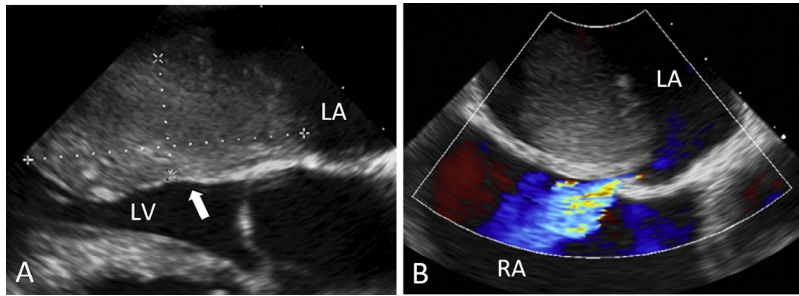


Fig. 2 – Transesophageal echocardiogram. (A) Gray-scale ultrasound image showing the heterogeneous left atrial mass as it extends across the mitral valve (arrow). **(B)** Color Doppler image again showing the atrial septal defect with left-to-right blood flow through the patent foramen ovale. LA, left atrium; LV, left ventricle; RA, right atrium.

however, the mass would need to be surgically removed due to the risks of embolic stroke or sudden cardiac death from obstruction. Plans were subsequently made to proceed with surgery. The patient underwent robot-assisted tumor resection and septal repair without complication. Histologic examination confirmed the diagnosis of an atrial myxoma (Fig. 4A and 4B).

The patient was seen several months following her procedure and reported that she was doing well. Although she did have some residual pain at her surgical site, she was walking several miles daily without dyspnea. Repeat TTE showed

postsurgical changes of the interatrial septum without a recurrent mass or persistent PFO.

Discussion

Primary cardiac tumors are rare, with an estimated prevalence between 0.001% and 0.25% of the population on autopsy studies [4]. Myxomas make up the majority of these, affecting women slightly more than men [5].

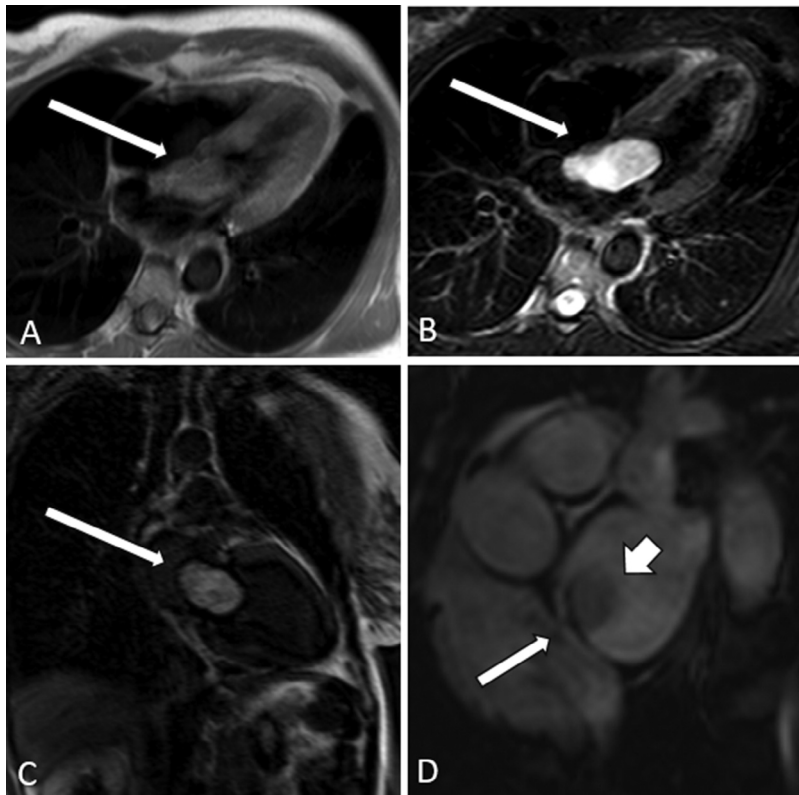


Fig. 3 – Cardiac magnetic resonance (CMR) imaging. (A) T1-weighted horizontal 4-chamber view showing predominantly isointense signal throughout the mass (arrow). **(B)** T2-weighted horizontal 4-chamber view showing that the mass is well-circumscribed, respecting tissue planes, and with high-intensity signal throughout (arrow). **(C)** Vertical long-axis late gadolinium-enhanced (LGE) view showing moderate heterogeneous enhancement throughout the mass (arrow). **(D)** Oblique gradient echo (GRE) view showing the mass (thick arrow) and relation to the patent foramen ovale (thin arrow).

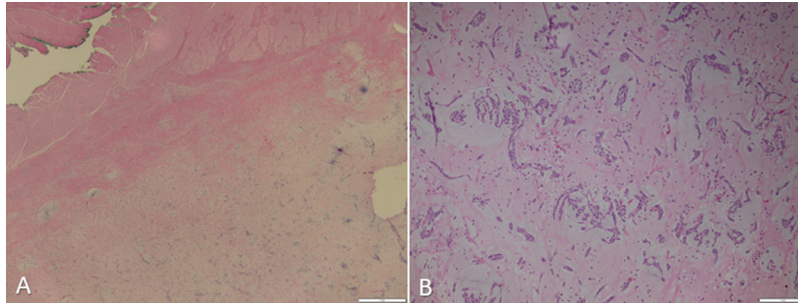


Fig. 4 – Mass histology. (A) Low power micrograph shows interface of the tumor with normal myocardium. (B) High-power micrograph shows bland spindled cells with eosinophilic cytoplasm and abundant myxoid background.

Approximately 75% of myxomas originate in the left atrium, with only 20% in the right atrium, 4% in the ventricles, and a finite number occurring on the valves, pulmonary arteries or veins, and vena cava [2,6]. Myxomas grow rapidly to an average diameter of 5–6 cm, but can reach as large as 15 cm [7]. Most are attached to a broad-based stalk near the fossa ovalis on the interatrial septum (as in this case), although up to one-fourth are sessile [2,3]. These endocardial-based masses do not typically invade the underlying myocardium, but rather expand into the adjacent cardiac chamber [3,6]. Their surface is generally smooth, but can be myxoid or gelatinous, or villous or irregular with surface thrombosis, from which either tumor or thrombus may break off and embolize [2,3,7]. Microscopically, myxomas consist of multipotential mesenchymal cells that persist during embryologic cardiac septation, giving rise to endothelial cells, smooth muscle cells, angioblasts, fibroblasts, cartilage cells, and myoblasts [2]. These cells are surrounded by subendocardial blood vessels, a mucopolysaccharide-rich stroma, and the tumors inconsistently contain hemorrhage, calcifications, fibrosis, and glands [2,5]. The heterogeneous nature of these tumors can often make the imaging variable and difficult to interpret [8].

Most patients will present with at least 1 of the 3 classic clinical symptoms—cardiac obstruction, embolism, or constitutional symptoms [3]. Cardiac obstructive symptoms are the most common, and consist of dyspnea, orthopnea, peripheral edema, paroxysmal nocturnal dyspnea, syncope, or sudden death [2,3]. Embolism occurs in up to 40% of patients, affecting predominantly the central nervous system arteries, but virtually any organ can be involved [2,3]. Indeed, many myxomas are first diagnosed after the patient has suffered a stroke [7]. Constitutional symptoms are seen in up to one-third of patients, and consist of fatigue, fever, erythematous rash, arthralgia, myalgia, and weight loss [2,3]. These constitutional symptoms are likely due to a release of IL-6, and can be accompanied by laboratory abnormalities such as anemia, leukocytosis, and an elevated erythrocyte sedimentation rate or C-reactive protein [2,3]. This can make myxomas difficult to differentiate from other diseases such as rheumatological conditions, endocarditis, or malignancies [2,3]. These symptoms typically resolve after the tumor is removed [2]. Up to 20% of patients with myxomas remain asymptomatic and their tumors are incidentally discovered at autopsy [5].

Interestingly, though PFOs themselves are present in up to one-quarter of normal hearts at autopsy, the association of

either PFOs or ASDs with atrial myxomas (as demonstrated in our case) is exceedingly rare. According to a 1998 review by Tsukamoto et al., only 23 cases of either PFO or ASD associated with an atrial have been reported in the English literature, with only 8 of these attributed to PFOs alone [9]. Since then, our literature review reveals 15 additional cases of an atrial myxoma with a PFO reported, to include our own [10–23]. In fact, some of these cases have demonstrated profound clinical effects, such as right-to-left shunting, hypoxemia, and even cryptogenic pulmonary emboli caused by tumor prolapse left-to-right through the PFO and subsequent immune and surface-mediated thrombogenesis [10,12].

Occasionally myxomas occur due to familial conditions such as LAMB (lentiginos, atrial myxoma, mucocutaneous myxoma, and blue naevi) and NAME (naevi, atrial myxoma, myxoid neurofibroma, and ephelides) syndromes, as well as the Carney complex [6]. The Carney complex is an autosomal dominant complex due to a mutation in the tumor suppressor gene *PRKAR1A* (protein kinase A regulatory subunit-1- α gene) on chromosome 17q22–24 [7]. It occurs in approximately 7% of myxomas and consists of both cardiac and extracardiac myxomas (such as skin and breast), hyperpigmented skin lesions, as well as other tumors (eg, pituitary adenomas and testicular tumors) [2,4]. It tends to occur more often in men, at younger ages (mean age of 24 years old), and is more likely to be multicentric (45%) and recurrent (22% vs 3% in typical sporadic myxomas) [5].

On physical examination, a friction rub or murmur (diastolic or systolic) may be auscultated, in addition to a characteristic “tumor plop,” neither of which was described in our case [2]. ECG usually demonstrates normal sinus rhythm, although arrhythmias such as atrial fibrillation or atrial flutter occur in up to 20% of cases [3,5]. Radiological evaluation most often begins with a chest radiograph, which can be normal in up to one-third of patients, but may demonstrate cardiomegaly, left atrial enlargement, pulmonary artery enlargement, pleural effusions, or rare calcifications [3,5]. TTE usually follows as part of the initial evaluation, but due to its limitations as described above, is frequently followed by TEE for a more complete assessment [3]. TEE can demonstrate the site of insertion and other surface features of the myxoma, as well as hemorrhage, necrosis, cysts, and calcifications [2]. It is limited, however, in making a global assessment of both cardiac and extracardiac structures. Coronary angiography is useful in patients over 40 years old to rule out concomitant coronary artery disease, as

well as to identify which blood vessels supply the tumor [2]. However, given that most cardiac lesions are not easily biopsied, additional imaging (such as CMR) is extremely useful to differentiate myxomas from other cardiac masses and to guide further management [8].

CMR offers several distinct advantages over the previously discussed imaging modalities. With respect to general anatomy, its multiplanar imaging and wide fields of view allow better determination of location, size, points of attachment, mobility, functional impact on valves, and involvement of myocardium and adjacent structures [2,3,5,8,24]. Detailing these features can inform surgical planning, such as whether a valve or septum needs to be repaired or replaced, and which approach would be most optimal [5–7]. Furthermore, due to particular signal patterns on T1- and T2-weighted imaging, it offers superior spatial and contrast resolution to better characterize soft tissues (eg, solid, liquid, hemorrhage, fat). This can help differentiate between malignancy, thrombus, and anatomic abnormalities [1–3,24]. Normal structures, such as the Coumadin ridge, Eustachian valve, Chiari network, right ventricular moderator band, and false left ventricular tendons, sometimes appear as suspicious masses on echocardiogram, but are easily characterized on CMR [1]. Gadolinium contrast allows even better tissue differentiation of masses from surrounding myocardium and determination of vascularity and tissue invasion if present. The ability to perform these functions to better assist in surgical planning without the use of ionizing radiation makes CMR a preferred imaging modality, particularly in children [24].

Limitations of CMR include technical challenges with gating and breath holding, as well as limitations shared by all magnetic resonance imaging, such as implanted metal or pacemakers, obesity, claustrophobia, and end-stage renal disease, which limits the use of gadolinium [24]. Cardiac CT can offer an alternative to CMR in some of these situations but is not discussed further here [24].

Typical protocols of CMR include some combination of black-blood T1-weighted (with and without contrast and fat suppression), black-blood T2-weighted, and early and late gadolinium-enhanced imaging [1]. These protocols are adapted to accommodate the variations in appearance and location of individual tumors to ensure the optimal imaging planes and sequences are acquired, thereby improving differentiation from other cardiac masses [8].

Due to their polysaccharide-rich ground substance and high extracellular water content, myxomas typically appear isointense or hypointense on T1-weighted imaging and hyperintense on T2-weighted imaging [1,4,5]. These tumors also enhance readily with gadolinium, which is particularly useful in differentiating myxomas from other common cardiac masses, such as thrombi, which do not enhance [4]. However, given the variable presence of hemorrhage, calcifications, surface thrombus, cystic degeneration, and fibrosis in these tumors, this enhancement is often heterogeneous [1]. For example, calcifications do not enhance and display low-signal intensity on both T1- and T2-weighting imaging, whereas inflammation enhances readily [5]. Necrosis and cystic degeneration do not enhance. Hemorrhage begins hypointense on both T1- and T2-weighted imaging and becomes increasingly hyperintense with age as the hemoglobin is oxidized to methemoglobin [1]. In

addition, this heterogeneous enhancement may increase 10 minutes after the administration of gadolinium with late gadolinium-enhanced sequences [8]. Because of this heterogeneous enhancement, these tumors can be difficult to distinguish from malignancy, if it were not that CMR can also demonstrate a lack of adjacent tissue invasion.

CMR generally performs better than echocardiography at distinguishing myxomas from thrombi and other cardiac lesions [8]. Acute thrombi, the leading alternative diagnosis, are generally isointense on T1- and T2-weighted imaging [1]. As they age and become more organized, they gradually lose their water content, and their methemoglobin-rich cellular debris is replaced by fibrous tissue, creating a uniformly lower signal intensity [1,8]. Although generally immobile and attached to the atrial wall by a broad base, they can become mobile, which makes them difficult to distinguish from myxomas [2]. This can be resolved with gadolinium contrast, as thrombus is avascular and does not enhance (the caveat being organized thrombus may enhance peripherally due to its fibrous makeup) [1,8]. Although not discussed in full detail here, other benign lesions can often be differentiated based on their location, size, signal intensities, and contrast enhancement. For instance, fibroelastomas, another common benign tumor, are more often valvular, smaller in size, contain a narrow stalk, and display low T1-weighted and high T2-weighted signal intensities [2,4,5,8]. Furthermore, they enhance homogeneously with contrast, as opposed to the heterogeneous enhancement of myxomas discussed earlier [8].

Features suggestive of a malignant lesion include strong contrast enhancement on T1-weighted images, invasion of adjacent and extracardiac structures, size greater than 5 cm, irregular and ill-defined borders, involvement of the right heart, multiple lesions, heterogeneous signal intensity, and hemorrhagic pericardial effusions [1]. Using these characteristics to diagnose malignant lesions, CMR carries a diagnostic accuracy (area under the curve) of 0.92 [1].

As previously mentioned, multiple imaging modalities play a role in the diagnosis and therapeutic decision-making process for cardiac masses. Features such as tumor type, location, valvular and myocardial involvement, comorbidities (eg, coronary artery disease), and patient age all play a role in determining the most appropriate surgical technique [6]. Regardless, the definitive treatment for all cardiac tumors is surgical removal, given the high risks of cardiac chamber obstruction and embolization (up to 10% of patients have been reported to die of embolization while awaiting operation) [9]. Most patients have good surgical outcomes, and less than 5% of nonfamilial myxomas are known to recur [4].

Acknowledgment

We would like to acknowledge the patient for allowing us to discuss her case with the academic community.

Supplementary data

Supplementary data associated with this article can be found online version, at <http://dx.doi.org/10.1016/j.radcr.2017.07.001>.

REFERENCES

- [1] Motwani M, Kidambi A, Herzog BA, Uddin A, Greenwood JP, Plein S. MR imaging of cardiac tumors and masses: a review of methods and clinical applications. *Radiology* 2013;268(1):26–43.
- [2] Reynen K. Cardiac myxomas. *N Engl J Med* 1995;333(24):1610–7.
- [3] Grebenc ML, Rosado de Christenson ML, Burke AP, Green CE, Galvin JR. Primary cardiac and pericardial neoplasms: radiologic-pathologic correlation. *Radiographics* 2000;20(4):1073–103, quiz 110–1, 112.
- [4] Malik SB, Kwan D, Shah AB, Hsu JY. The right atrium: gateway to the heart—atomic and pathologic imaging findings. *Radiographics* 2015;35(1):14–31.
- [5] Grebenc ML, Rosado-de-Christenson ML, Green CE, Burke AP, Galvin JR. Cardiac myxoma: imaging features in 83 patients. *Radiographics* 2002;22(3):673–89.
- [6] Buckley O, Madan R, Kwong R, Rybicki FJ, Hunsaker A. Cardiac masses, part 2: key imaging features for diagnosis and surgical planning. *AJR Am J Roentgenol* 2011;197(5):W842–51.
- [7] Hoffmeier A, Sindermann JR, Scheld HH, Martens S. Cardiac tumors—diagnosis and surgical treatment. *Dtsch Arztebl Int* 2014;111(12):205–11.
- [8] Abbas A, Garfath-Cox KA, Brown IW, Shambrook JS, Peebles CR, Harden SP. Cardiac MR assessment of cardiac myxomas. *Br J Radiol* 2015;88(1045):20140599.
- [9] Tsukamoto S, Shiono M, Orime Y, Hata H, Yagi S, Kimura S, et al. Left atrial myxoma with an atrial septal defect: a case report and review of the literature. *Ann Thorac Cardiovasc Surg* 1998;4(3):133–7.
- [10] De Vry DJ, Ferron DR, Kersten JR, Rashid ZA, Pagel PS. How can a large left atrial myxoma cause a selective mid-diastolic right-to-left atrial shunt? *J Cardiothorac Vasc Anesth* 2015;29(3):820–3.
- [11] Gonzalez-Ferrer JJ, Carnero M, Labayru VL, de Isla LP, Zamorano JL. Left atrial myxoma prolapsing through the foramen ovale. *Eur J Echocardiogr* 2008;9(4):595–7.
- [12] Kimura K, Jezumi Y, Noma S, Fukuda K. Left to right protrusion of a left atrial myxoma through a patent foramen ovale in a patient with “cryptogenic” pulmonary embolism. *Eur Heart J* 2010;31(10):1247.
- [13] Lasam G, Ramirez R. Concomitant left atrial myxoma and patent foramen ovale: is it an evolutionary synergy for a cerebrovascular event? *Cardiol Res* 2017;8(1):26–9.
- [14] Molnar A, Encica S, Sacui DM, Muresan I, Trifan AC. A very rare association between giant right atrial myxoma and patent foramen ovale. Extracellular matrix and morphological aspects: a case report. *Rom J Morphol Embryol* 2016;57(2):573–7.
- [15] Roque J, Silva F, Arruda Pereira R, Cravino J. Multiple causes for an ischemic stroke: myxoma, papillary fibroelastomas and patent foramen ovale. *HSR Proc Intensive Care Cardiovasc Anesth* 2012;4(3):187–91.
- [16] Saaidi I, Khalifa S, Makni H, Mokaddem A, Boujnah MR. [Right atrial myxoma associated with a patent foramen ovale revealed by recurrent strokes]. *Tunis Med* 2008;86(1):83–4.
- [17] Sabzi F, Faraji R. Preoperative emboli in a pregnant woman with myxoma. *Iran J Med Sci* 2016;41(4):345–9.
- [18] Saitoh H, Kubota H, Takeshita M, Mizuno A, Suzuki M. Right atrial myxoma with right to left shunt and coronary artery disease. *Jpn Circ J* 1994;58(1):76–9.
- [19] Simoes O, Loureiro MJ, Miranda R, Lopes L, Almeida S, Cordeiro P, et al. Left atrial myxoma associated with severe mitral regurgitation and patent foramen ovale. *Rev Port Cardiol* 2007;26(4):447–9.
- [20] Tondelli M, Mandrioli J, Ficarra G, Pentore R, Girolami F, Ghidoni I, et al. Teaching NeuroImage: when right atrial myxoma meets patent foramen ovale: a case of paradoxical brain embolism. *Neurology* 2008;70(1):e1–2.
- [21] Umana E, Alpert MA, Massey CV, Tucker JA, Damrich ME. Biatrial myxoma resembling an interatrial clot in transit on echocardiogram. *South Med J* 1999;92(10):1019–22.
- [22] Van Malderen S, Kerkhove D, Tanaka K, Van Hecke W, Van Camp G. Paradoxical embolism in a patient with a large tricuspid myxoma and patent foramen ovale. *Eur J Echocardiogr* 2011;12(8):641.
- [23] Vivo RP, Krim SR, Dela Cruz JD, Ramchandani M, Shah DJ, Little SH, et al. Multimodality imaging of giant prolapsing left atrial myxoma. *Methodist DeBaakey Cardiovasc J* 2010;6(2):40–2.
- [24] Buckley O, Madan R, Kwong R, Rybicki FJ, Hunsaker A. Cardiac masses, part 1: imaging strategies and technical considerations. *AJR Am J Roentgenol* 2011;197(5):W837–41.